Exploring Aerodynamic forces on 3D Printed Propellers

Adam Deeley
Physics Department, The College of Wooster, Wooster, Ohio 44691, USA
(Dated: May 9, 2019)

In order to test efficiencies and forces acting on propellers, two different propellers were designed and 3D printed. They were tested at various blade orientations (number of blades) and they were given different airfoil cross sections, one a NACA M10, the other an AH-85-L-120/17. It was found that that the NACA propellers generated more lift and had a better lift to drag ratio, making them more efficient than the other airfoil.

INTRODUCTION

A propeller works as a driving force for vehicles due to the lift forces generated by its design. A propeller's cross section is defined as an airfoil, as it is placed in an airstream to produce an aerodynamic force in the most efficient manner possible [1]. There are many factors that go into the design of a propeller, such as the profile of the airfoil cross section and the angle of attack, which are in turn determined by other factors, such as rotational speed, length of blade, and airflow velocity. As far as the airfoil is concerned, the design of the cross section is characterized mainly by the chord, camber, and thickness, shown in Figure 1. Described in source [1], the chord line is a straight line which connects the leading and trailing edge, while the chord is the distance between the edges along the chord line. The mean camber line is halfway between the upper and lower curve, following the average of the curves. The camber is the maximum distance between the mean camber line and the chord line. These features are varied between propellers based on the conditions it is likely to face. Of the external conditions, the velocity of the fluid which the propeller travels in is arguably the most important. The is because the velocity is directly related to the angle of attack, which in turn directly affects the thrust generated by a propeller. The angle of attack is the angle between the chord line and the relative velocity experienced by the propellers. As a propeller moves through a fluid, the fluid's velocity moves perpendicular to the disk created as the propellers rotate, and the fluid also moves parallel to the blade, shown in Fig. 2 by the rotational relative wind and the induced flow, respectively. By resolving the vectors, a relative velocity is found, from which the angle of attack is found.

In this experiment we will investigate the lift and drag experienced by two different styles of propeller, with airfoil profiles NACA M10 and AH-85-L-120/17. The drag will be studied using an Ealing air gyroscope and the thrust will be investigated using a frictionless cart and spring. The study will look at the two styles for 2, 4, and 6 blades at low, medium, and high speeds of a box fan motor.

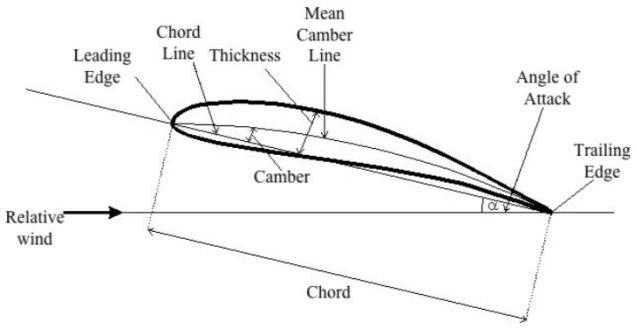

FIG. 1: Geometry of an Airfoil. The image is taken from source [1].

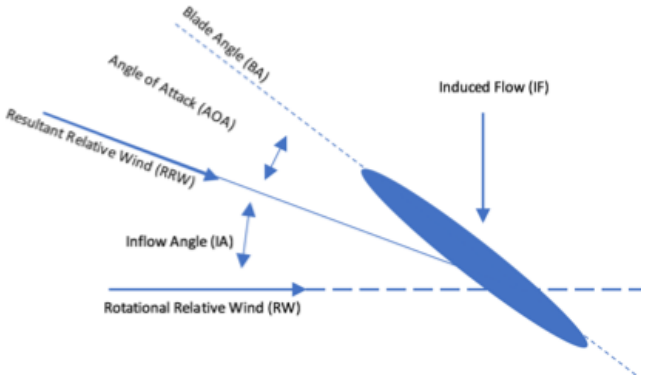

FIG. 2: Fluid flow experienced by an airfoil. The image is taken from source [2]

THEORY

A propeller experiences several forces, the two most important being the thrust, also called lift, and the drag, which can also be known as torque. Because a propeller is profiled from an airfoil, it follows similar principles to how an airfoil generates lift. There are several versions of lift theory, the most common misconception being that lift is generated as the airflow over the top curve of an airfoil travels faster to reach the tailing edge, due to the top curve being longer. This difference in speed creates a low pressure system above the airfoil, and the difference in pressure causes the airfoil to lift [3]. According

to source [2], lift is actually generated as airflow bends around the airfoil. As the airflow bends, the air in contact with the upper surface drags the air above it down to the surface, creating lower pressure system above the propeller. The difference in pressure here generates the lift force.

Blade Element Momentum Theory

While a propeller cross section does generate lift similarly to a wing with the same airfoil profile, it is quite a bit more complex than a wing. The forces which act on a propeller are defined in the Blade Element Momentum Theory (BEMT). Based off of the work of Rankine and Froude, BEMT combines two different theories, blade element theory and momentum theory. Blade element theory allows the blades to be divided into small elements of width dr which act independently and operate aerodynamically as two dimensional airfoils whose forces can be calculated based on local conditions [2]. The forces acting on these elements are then combined over a total radial distance to find the total force acting on the propeller. The second part, momentum theory, allows for the calculation of the induced velocities from vortices created by momentum lost in the flow. That is to say, that as the blades rotate through the fluid, there are vortices created in the wake of the propellers. The induced velocities of these vortices affect inflow of fluid through the propeller system and therefore the forces calculated by blade element theory [2]. By combining the two into BEMT, the blades can be divided into many small elements, which as they rotate trace out annular regions in which momentum balancing takes place.

Using this theory, we develop equations for the thrust

$$dT = B\frac{1}{2}\rho {V^2}_{total}\left(C_L\cos\phi + C_D\sin\phi\right)cdr, \qquad (1)$$

and drag dQ generated at each section of width dr.

$$dQ = B\frac{1}{2}\rho {V^2}_{total}\left(C_L\sin\phi - C_D\cos\phi\right)cdr, \qquad (2)$$

where dT and dQ are differentials of the thrust and drag, B is the number of blades, ρ is the density of air, V_{total} is the relative velocity of the airflow, ϕ is the angle of attack, c is the chord length and dr is a section of infinitesimal width. A detailed derivation for these equations can be found in source [2].

The only missing variables in the equations are the coefficients of drag and lift. The National Advisory Committee for Aeronautics (NACA) defines the lift coefficient as

$$C_L = \frac{T}{\rho n^2 D^4}. \qquad (3)$$

By inserting this into the equations and integrating them through the angle of attack and length of the blades, we can find the drag coefficient C_D. With the lift and drag coefficients, the propellers' efficiencies can be analyzed.

Because the propeller systems in this experiment are static, in that they do not translate through the fluid as they spin, the relative velocity is only the rotational relative velocity, and the angle of attack is then only the angle between the blade and this velocity. Keeping that in mind, the velocity of the fluid is the translational velocity of the blade elements as they travel through it. This allows us to substitute ${V^2}_{total} = \omega r$ into Eq. 1 and 2.

PROCEDURE

For this experiment, an Ealing air gyroscope was used. The gyroscope apparatus is connected to a tank of compressed nitrogen gas, and a steady flow of 4psi was output to the gyroscope apparatus to create a cushion of air for the rotor to sit on for each run. In order to study the angular velocity of the ball, four black strips of electrical tape are placed on the upper portion. (See Fig. 3.) The gyroscope was set up so that a laser reflected off of the ball, the beam passed through a lens which focused it onto a fast photodiode. Because the bottom of the tape was frayed on our rotor, the height of the incident beam from the laser was increased, and then the lens and photodiode were realigned to match the new beam path. The photodiode is connected to a Schmitt trigger, and when the laser light is incident on the photodiode, current passes through a phototransistor which triggers a voltage reading to pass through the Schmitt trigger. When the laser light is not hitting the photodiode, a low voltage reading is passed to the Schmitt trigger. The Schmitt trigger shapes the voltage signals into square waves, which can be seen in an attached oscilloscope and read by a frequency counter [4]. In order to ensure the photodiode was properly aligned with the laser, I connected the photodiode before the Schmitt trigger so that the oscilloscope displayed the intensity of the light. Adjusting the photodiode so that it received maximum intensity from the laser, I reconnected the photodiode to the Schmitt trigger. The frequency counter is connected to a Macintosh computer so that a LabView algorithm could import the data.

The LabView program set the controls for the frequency counter and calculated the average rotations per second over an interval of approximately 10 seconds. To analyze the data collected, it was exported to Igor Pro 8.

In addition to the Ealing air gyroscope, a stabilizing unit was built, shown in Fig. 4. The unit features a bearing that the shaft sits in to prevent it from tipping as the ball spun. There was no drag added by the bearing to the system. In order to spin the ball to the high rotations per minute of the fan motor which would be later used to test thrust, an adapter was designed and 3D printed so that a buffing pad could be used to spin the ball.

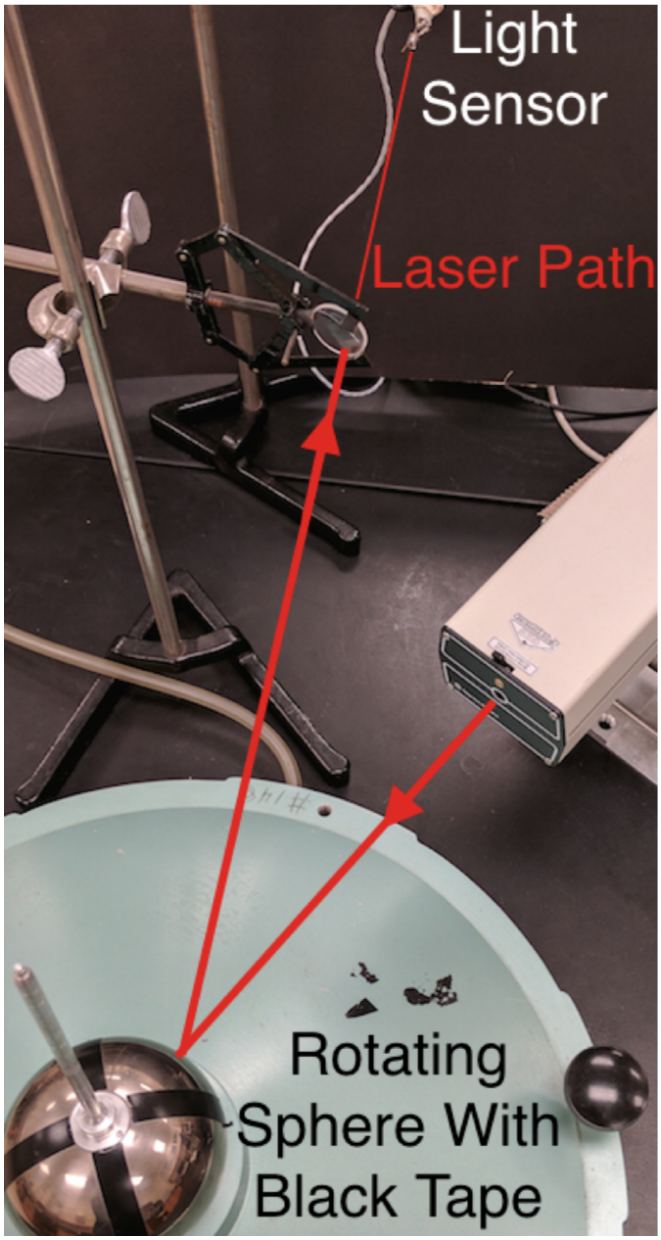

FIG. 3: Image of the gyroscope apparatus used in the experiment. The image is taken from source [5]

During the drag test, three different blade orientations were tested for two different styles of propeller. The propellers were designed in Fusion 360 and 3D printed on a Makerbot ReplicatorMini. The propellers are shown in Fig. 5 and 6 and they have a diameter of 23.6 cm, and the designs are shown in Fig 7 and 8.

In order to test for the thrust, a frictionless cart was used and a device was built so that the fan motor could be mounted to it. This equipment is shown in Fig. 9. The cart was placed on its track and attached to a spring of constant 3.267. The spring force would be equal to the thrust force and could then be determined by the distance

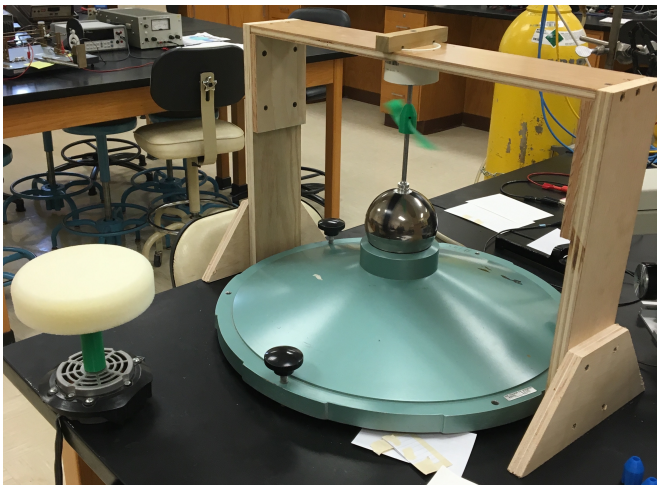

FIG. 4: An image of the apparatus which includes the addition of the stabilizing unit and fan motor.

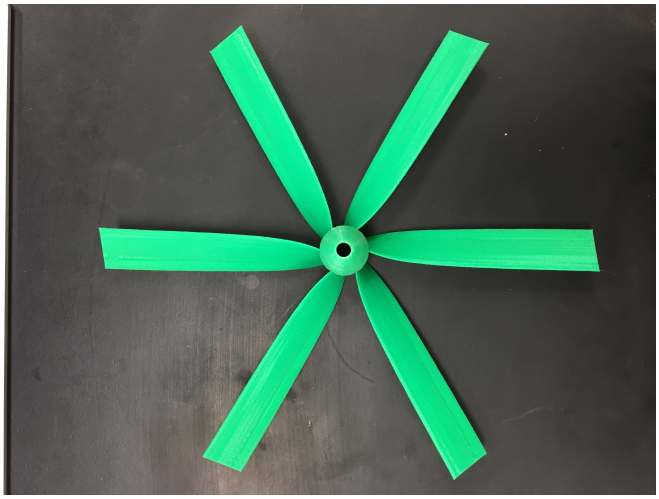

FIG. 5: Propeller with six blades.

the cart was displaced. In order to properly test for the thrust, the cart and track had to be placed so that the motor's cord did not add more resistive force to the cart's motion. Several trials per datapoint were taken to ensure the measurements were accurate.

DATA AND ANALYSIS

When analyzing the data from the drag test with the Ealing air gyroscope and comparing it to the BEMT, it became clear that the drag data taken did not quite fit with the drag and lift equations, because Newton's drag model and the BEMT define drag and the drag coefficients differently. Therefore, the drag data taken on the gryoscope would be plotted to show the difference in the degradation of angular speed caused by the drag . Actually acquiring the lift and drag coefficients, as well as

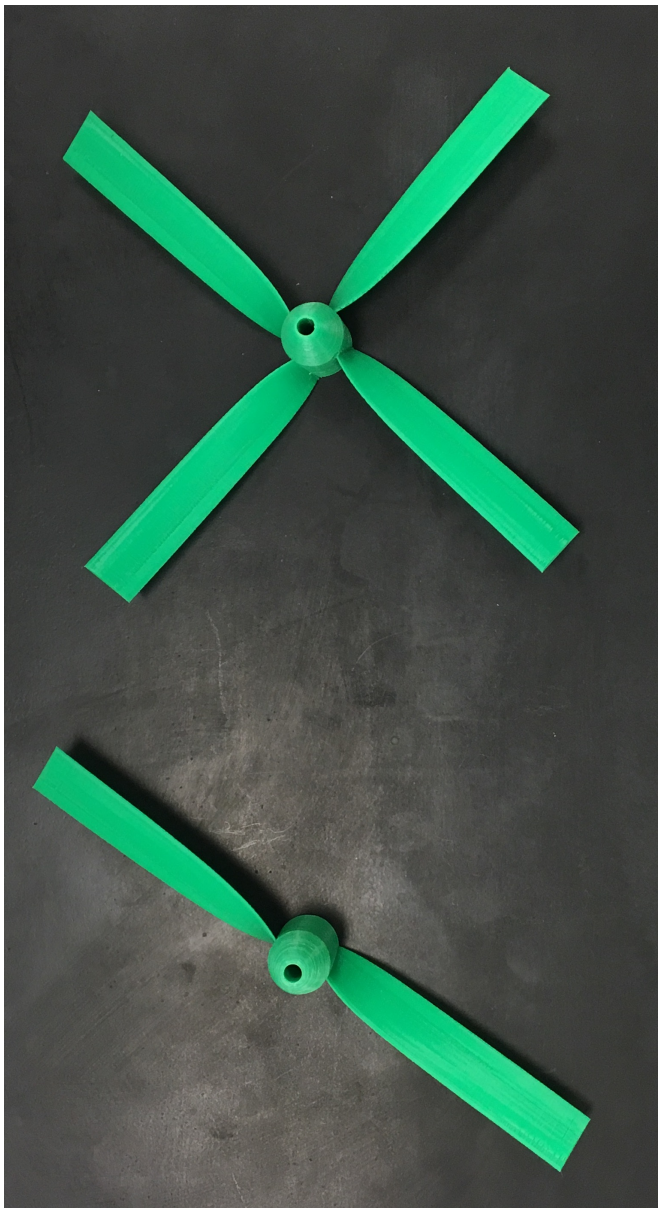

FIG. 6: Two and four bladed propellers.

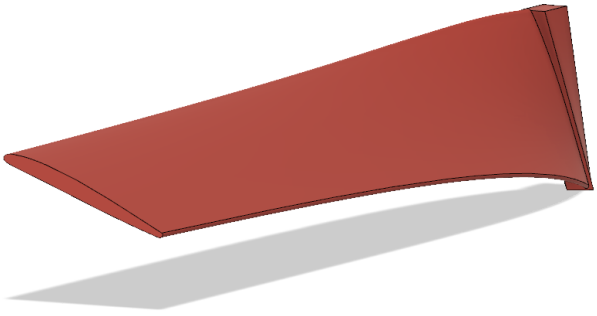

FIG. 7: Design of propeller with airfoil profile NACA M10.

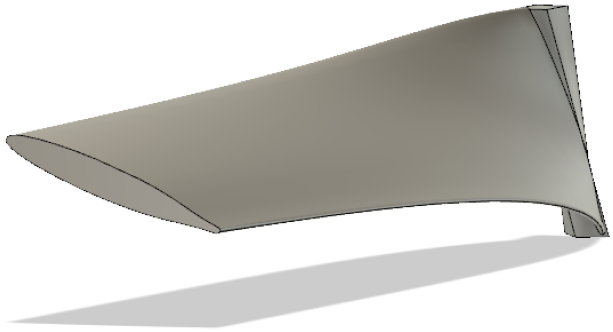

FIG. 8: Design for propeller with airfoil profile AH-85-L-120/17.

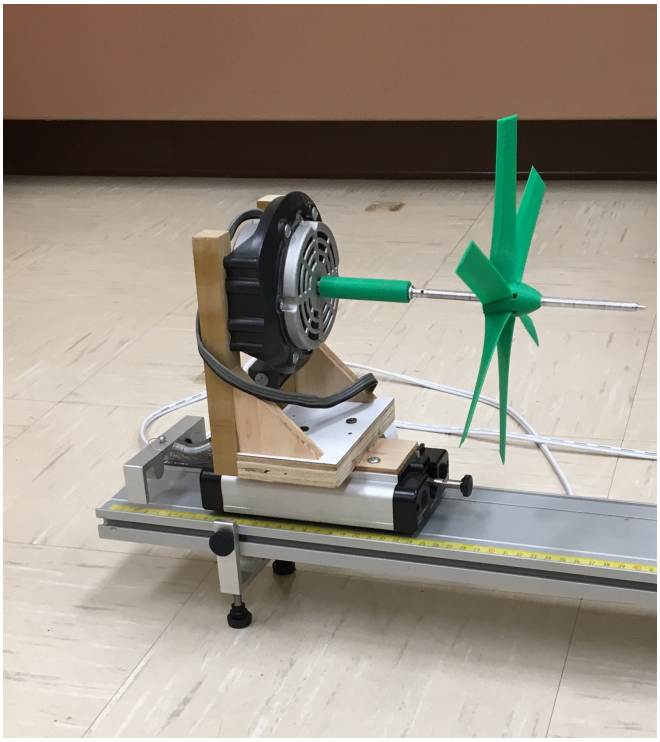

FIG. 9: Cart used for measuring thrust.

the drag itself, would have to come from the BEMT, and thus from this the thrust measurements. Using Eq. 3, one can find the values for the lift/thrust coefficient. Then, the lift coefficient can be input into Eq. 1, which can be rearranged to solve for the drag coefficient. The drag coefficient can then be inserted into Eq. 2 to solve for the drag. The drag data was taken for the different propellers at different rotations per minute, high, medium, and low. When plotted against each other, the data did not vary, so only the high rotational speed data values were used when comparing thrust and drag as a function of the number of blades.

The measured thrust values are plotted against the ro-

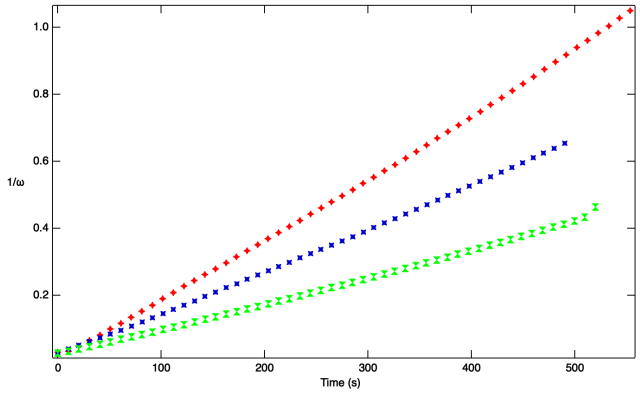

FIG. 10: Plot showing the difference in the drag coefficients. Green hourglasses represent 2 blades, blue stars represent four blades and red stars represent six blades. Because the propellers experience the same exponential decay despite their starting speed, only the high rpm data is shown.

tation rate in Fig. 11. The data shows that for each blade orientation, the NACA M10 generates higher thrust values than the AH-85-L-120/17. Fig. 12 shows the thrust and torque of the different propellers versus the number of blades. The two different profiles experience similar drag, but the NACA airfoil again generates more thrust than its counterpart compared to the drag generated.

CONCLUSIONS

The data show that the NACA M10 airfoil is more efficient than the AH-85-L-120/17 airfoil. It generates more thrust while maintaining a better thrust to drag ratio. Some changes that could be made with the experiment would be a battery powered motor to completely negate the effect of the fan motor cord on the thrust experiment. Also, a different, higher speed motor or motors with more speeds could be used. Another key point is that the experiment would be very different if the thrust and drag were not measured statically. By eliminating transverse movement, the only effective velocity acting on the blade is the airspeed which the propellers experience as they spin, there is no frontal, perpendicular velocity. This changes the angle of attack, which in turn affects how much thrust is generated. The derivation I used to obtain values for my data was only possible due to the propeller being static and not experiencing that other velocity.

ACKNOWLEDGEMENTS

I would like to thank Dr. Lehman and the College of Wooster Department of Physics for their help in setting up my graphs and in the web articles for helping me understand how to analyze my data. I would like to thank my father for the access to his shop and materials, and for teaching me the skills required to visualize and build what I needed.

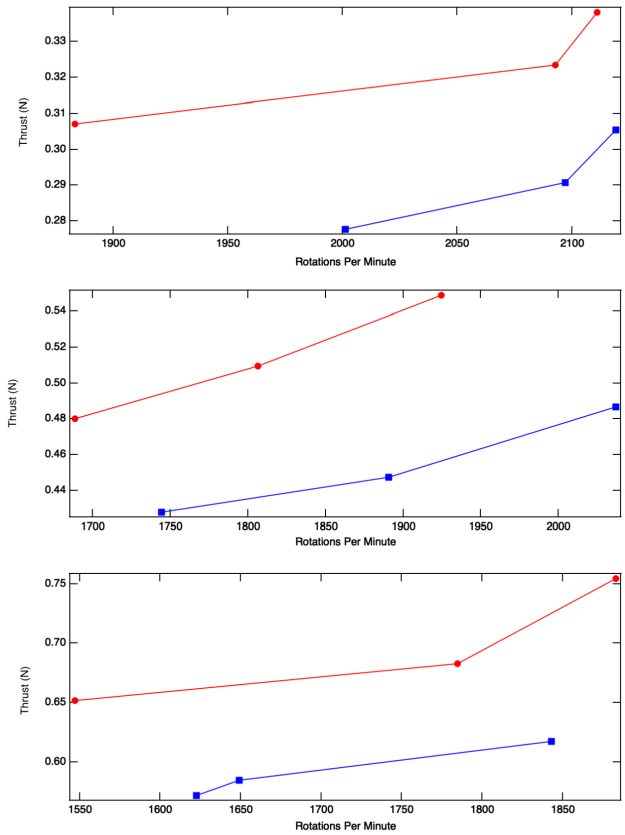

FIG. 11: Plots of the thrust of the propellers as a function of rotation speed. The NACA M10 propeller is represented by the red line with circular markers while the AH-85-L-120/17 propeller is represented with a blue line and square markers. a.) 2 Bladed propeller data b.) 6 Bladed propeller data c.) 4 bladed propeller data.

[1] Sullivan, Alex. "Aerodynamic Forces Acting on an Airfoil." Department of Physics, The College of Wooster, 2010.
[2] P.J. Moriarty, A.C. Hansen, "AeroDyn Theory Manual", NREL/TP-500-36881, 2005.
[3] W. L. LePage, *The ABC of Flight*, John Wiley & Sons, Inc., New York, 1982.
[4] Grugel, Manon E. "Modeling the Viscous Torque Acting on a Rotating Object." Department of Physics, The College of Wooster, 1998.
[5] Vajpeyi, Avi, "Stokes' and Newton's Viscous Drag." Department of Physics, The College of Wooster, 2017.
[6] Rachit Prasad, Seongim Choi "Variable-fidelity aerodynamic analysis of lift fan type aircraft." Aerospace Science and Technology, Vol. 71, 636-650, 2017.
[7] *Junior I.S. Lab Manual*, The College of Wooster, (2018).

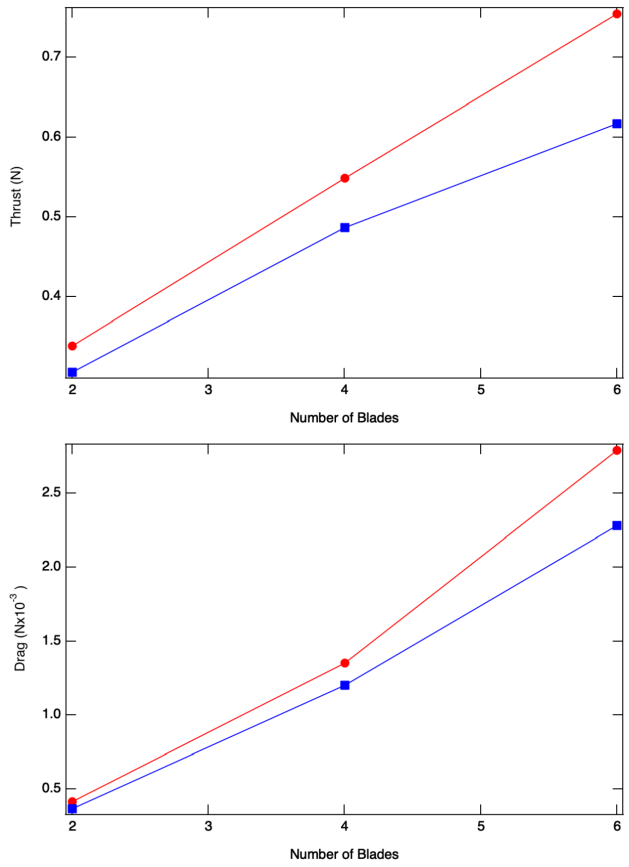

FIG. 12: Comparison of a.) the thrust and b.) the torque for the two airfoil profiles as a function of the number of blades in the propeller. The NACA M10 propeller is represented by the red line with circular markers while the AH-85-L-120/17 propeller is represented with a blue line and square markers.